Res Chem Intermed (2016) 42:571–580
DOI 10.1007/s11164-015-2042-1

Comprehensive monitoring of the performance of homogenous and heterogeneous UV/H_2O_2/$S_2O_8^{2-}$/Fe^{2+} processes in mineralization of Acid Red 73

Alireza Khataee[1] · Hamid Aleboyeh[2] · Mohsen Sheydaei[3] · Azam Aleboyeh[2]

Received: 13 December 2014 / Accepted: 2 April 2015 / Published online: 17 April 2015

Abstract Degradation of an azo dye, Acid Red 73 (AR73), was examined in detail using the UV/H_2O_2/$S_2O_8^{2-}$/Fe^{2+} process. UV–Vis absorbance, total organic carbon, H_2O_2 concentration, and pH of solution were monitored during the mineralization process. The results indicated that the mineralization efficiency was optimized from 78.8 to 95.6 % as a result of increasing the initial concentration of $S_2O_8^{2-}$ from 0.923 to 3.70 mM. The capability of this process was compared with those of UV/H_2O_2, UV/H_2O_2/Fe^{2+}, and UV/H_2O_2/$S_2O_8^{2-}$ processes. The UV/H_2O_2/$S_2O_8^{2-}$/Fe^{2+} process was more effective than other processes in degradation of AR73. Moreover, Fe^{2+} was immobilized on the surface of zeolite (ZSM5), and its immobilization effect was examined. Mineralization efficiency in the Fe^{2+} catalyzed process was higher than that of the Fe^{2+}–ZSM5 catalyzed process.

Keywords Advanced oxidation processes · Degradation · Monitoring · Textile dye · Zeolite

Introduction

Organic dyes are one of the largest groups of pollutants in wastewater produced from textiles and various branches of other industries. The discharge of these highly colored effluents into the aquatic environment can cause problems because of the introduction of large quantities of chemical oxygen demand, non-biodegradable

✉ Alireza Khataee
a_khataee@tabrizu.ac.ir; ar_khataee@yahoo.com

[1] Research Laboratory of Advanced Water and Wastewater Treatment Processes, Department of Applied Chemistry, Faculty of Chemistry, University of Tabriz, 51666-16471 Tabriz, Iran

[2] Laboratoire de Génie des procédés des effluents, Ecole Nationale Supérieure de Chimie de Mulhouse, Université de Haute-Alsace, 3, rue Alfred Werner, 68093 Mulhouse Cedex, France

[3] Faculty of Chemistry, Kharazmi University, 15719-14911 Tehran, Iran

organics, and other hazardous chemicals [1, 2]. Furthermore, dyes may significantly affect photosynthetic activity in aquatic life because of reduced light penetration. Therefore, it is necessary to remove these pollutants from waste effluents. Various methods of treatment were developed and utilized to remove these pollutants from aqueous media. One category of available and promising method is the advanced oxidation processes (AOPs) [3]. AOPs refer to the processes aimed at generating reactive radicals for oxidative degradation of persistent hazardous organic pollutants or their transformation into less toxic intermediates [4]. The reactive radicals can be developed through the activation of strong oxidants under electrical, chemical, or radioactive energy in the presence of homogeneous or heterogeneous catalysts [5].

Among the various AOPs, the Fenton process is widely used for the successful remediation of non-biodegradable pollutants, especially pesticides, dyes, and phenolic contaminants [6–8]. In this simple and environmentally friendly process, reactive radicals are developed from catalytic degradation of hydrogen peroxide in the presence of the Fe^{2+} ion as catalyst [9]. This process is illustrated in reaction (1):

$$Fe^{2+} + H_2O_2 \rightarrow Fe^{3+} + {}^{\cdot}OH + OH^- \quad (1)$$

Fe^{2+} after being oxidized into Fe^{3+} can be regenerated through the reaction of Fe^{3+} by H_2O_2 as illustrated in reaction (2), [10]:

$$Fe^{3+} + H_2O_2 \rightarrow Fe^{2+} + HO_2^{\cdot} + H^+ \quad (2)$$

However, the Fenton process suffers from some operational problems. The basic problem is the slow regeneration of $Fe^{2+,}$ which leads to the decrease in overall oxidation rate in this process [11]. In addition, the Fe^{3+} ions may generate stable complexes with carboxylic acids, which inhibit complete degradation of pollutants and iron activity [1]. One more limitation of the Fenton reaction is the scavenger effect of highly concentrated $H_2O_{2,}$ which limits the effective concentration of this oxidant. Consequently, numerous efforts have been recently made to enhance the merits of the Fenton process and eliminate its drawbacks. One of the promising procedures is the application of ultraviolet (UV) irradiation with the Fenton process called the photo-Fenton process. In the presence of UV irradiation, Fe^{3+}–carboxylic acid complexes are degraded and free Fe^{3+} is reduced to form Fe^{2+} as illustrated in reactions (3, 4) [12].

$$Fe^{3+} + H_2O + hv \rightarrow Fe^{2+} + {}^{\cdot}OH + H^+ \quad (3)$$

$$Fe(OOC - R)^{2+} + hv \rightarrow Fe^{2+} + R^{\cdot} + CO_2 \quad (4)$$

The application of additional inorganic oxidants accompanied with hydrogen peroxide is another procedure, which has been recently used to improve the performance of the Fenton reaction. These oxidants including persulfate enhance the generation of different radicals for oxidative degradation of organic contaminants. Another amendment and modification of the Fenton process involves controlling the amount of iron in the solution by applying heterogeneous iron

sources. In this process, iron oxide particles or Fe ions can be immobilized on the surface of different solids and react with H_2O_2 to form a reactive radical hydroxyl.

The purpose of the present work is to improve the performance the photo-Fenton reaction with the accompanying inorganic oxidants such as H_2O_2 and persulfate and to monitor the decolorization and mineralization of a model pollutant, Acid Red 73 (AR73), comprehensively for the first time. The ability of the UV/H_2O_2/$S_2O_8^{2-}$/Fe^{2+} process in degradation of AR73 was compared with that of UV/H_2O_2, UV/H_2O_2/Fe^{2+}, and UV/H_2O_2/$S_2O_8^{2-}$ processes. Furthermore, the present work aimed at providing insight into the effect of operating parameters, such as persulfate concentration, H_2O_2 concentration, and pH. Moreover, Fe^{2+} was immobilized on the surface of zeolite (ZSM5), and its immobilization effect was investigated on the catalytic performance of this cation.

Experimental section

Materials

Acid Red 73 (MW = 556.49 g/mol) was obtained from Sigma Aldrich as a commercially available dye and was used without further purification. Hydrogen peroxide (30.7 % W/V, Fisher Chemical), potassium persulfate 98 % (Fluka Co.), and also $FeSO_4$. $7H_2O$ (Prolobo Co.) were used. All other chemicals were of the analytical grade. Distilled water was used throughout the investigation.

Photochemical treatment procedure

The photochemical reactor consisted of a tubular closed circulation batch vessel and a low-pressure mercury lamp (Philips, 15 W, 253.7 nm) in the center. The thickness of the colored solution surrounding the lamp was 1.4 cm. The AR73 solution with the concentration of 0.1 mM was injected from the bottom of the reactor (volume of the treated solution was 2 L) with a flow rate of 3.2 L/min. The incident energy of the lamp on the surface of the quartz tube was measured by a Lutron UV radiometer (27 W/m^2).

Analysis methods

At the defined time interval in the degradation reaction, the AR73 concentration was determined by using a Jasco (V-530) UV/Vis spectrophotometer at the characteristic wavelength of the dye solution (λ_{max} = 509 nm) to follow the progress of the decolorization during the process. Prior to the measurement, calibration curves were obtained using the solutions with the known concentrations of the dye, which indicated a significant linear relationship between absorbance and dye concentration up to 10^{-4} M. Decolorization efficiency (%) was equal to $[1 - C_t/C_0] \times 100$, where C_0 denotes the initial concentration of AR73 solution and C_t refers to its concentration after a certain time (t) of reaction.

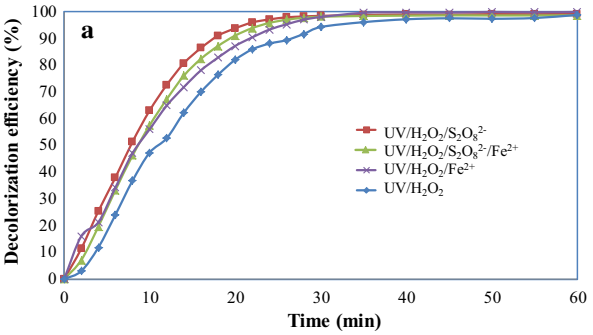
a
Decolorization efficiency (%)
Time (min)
UV/H2O2/S2O8 2-
UV/H2O2/S2O8 2-/Fe2+
UV/H2O2/Fe2+
UV/H2O2

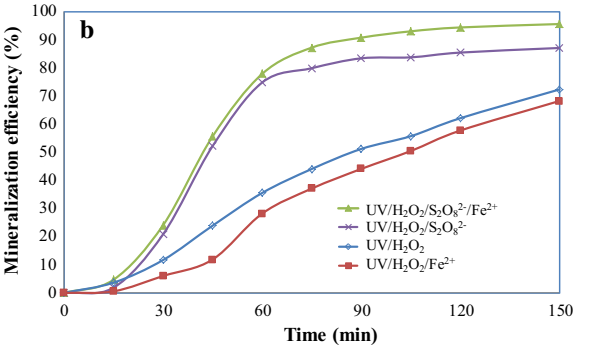
b
Mineralization efficiency (%)
Time (min)
UV/H2O2/S2O8 2-/Fe2+
UV/H2O2/S2O8 2-
UV/H2O2
UV/H2O2/Fe2+

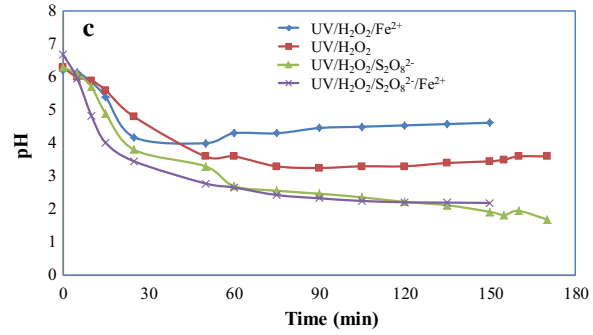
c
pH
Time (min)
UV/H2O2/Fe2+
UV/H2O2
UV/H2O2/S2O8 2-
UV/H2O2/S2O8 2-/Fe2+

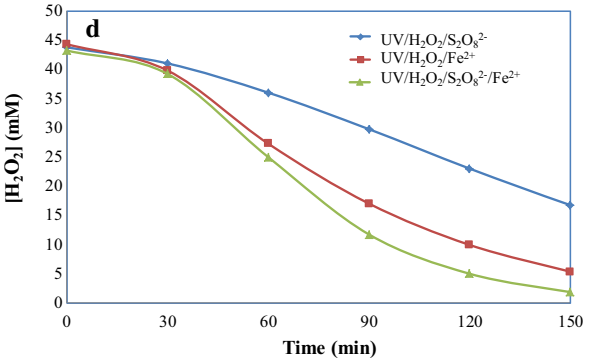
d
[H2O2] (mM)
Time (min)
UV/H2O2/S2O8 2-
UV/H2O2/Fe2+
UV/H2O2/S2O8 2-/Fe2+

◀**Fig. 1** Variation of **a** decolorization efficiency, **b** mineralization efficiency, **c** pH of solution, and **d** H_2O_2 concentration during the treatment of AR73 solution by UV/H_2O_2, UV/H_2O_2/Fe^{2+}, UV/H_2O_2/$S_2O_8^{2-}$ and UV/H_2O_2/$S_2O_8^{2-}$/Fe^{2+} processes in the presence of $[AR73]_0 = 0.1$ mM, $[H_2O_2]_0 = 44.4$ mM, $[Fe^{2+}]_0 = 2.43$ mg/L and $[S_2O_8^{2-}]_0 = 1.84$ mM

A Shimadzu Tocvcsn analyzer was used to determine the extent of dye mineralization on the bases of total organic carbon (TOC) measurements. Mineralization efficiency was equal to $[(1 - TOC_t/TOC_0] \times 100$, where TOC_0 refers to the initial TOC of AR73 solution and TOC_t stands for the same parameter at time t. The residual of H_2O_2 was monitored by 0.04 M potassium permanganate at an acidic condition [13]. The solution pH was monitored using a Consort C863 pH meter.

Immobilization of Fe^{2+} on a ZSM5 surface

The method described by Kasiri et al. [14] was used to immobilize Fe^{2+} on the surface of ZSM5. Accordingly, silica and iron sources were solubilized by fluoride ions. Then Fe^{2+}–ZSM5 was synthesized at the temperature of 90 °C and calcined at 550 °C. The surface area of the prepared Fe^{2+}–ZSM5 composite was 187 m^2/g. This composite included Si, S, Mn, Fe, and O elements with 44.692, 0.011, 0.036, 3.070, and 52.1 wt%, respectively.

Results and discussion

Comparing the degradation abilities of UV/H_2O_2, UV/H_2O_2/Fe^{2+}, UV/H_2O_2/$S_2O_8^{2-}$ and UV/H_2O_2/$S_2O_8^{2-}$/Fe^{2+} processes

In this study, the abilities of UV/H_2O_2, UV/H_2O_2/Fe^{2+}, UV/H_2O_2/$S_2O_8^{2-}$ and UV/H_2O_2/$S_2O_8^{2-}$/Fe^{2+} processes for degradation of AR73 were compared with each other. The following experimental conditions were used to conduct experiments: initial dye, H_2O_2, Fe^{2+} and $S_2O_8^{2-}$ concentrations of 0.1 mM, 44.4 mM, 2.43 mg/L, and 1.84 mM, respectively. As illustrated in Fig. 1, the variation in decolorization and mineralization efficiencies, solution pH, and H_2O_2 concentration during the degradation processes were measured. Figure 1a indicates that all the four processes were efficient in decolorization of AR73. It may be due to the fast effect of produced radicals through the all mentioned processes on cleavage of azo bonds and subsequent rapid decolorization. According to Fig. 1b, the mineralization efficiency can be ranked as: UV/H_2O_2/$S_2O_8^{2-}$/Fe^{2+}> UV/H_2O_2/$S_2O_8^{2-}$>UV/H_2O_2 > UV/H_2O_2/Fe^{2+}.

The mechanisms proposed for UV/H_2O_2 [1, 15–17], UV/H_2O_2/$S_2O_8^{2-}$ [15, 18–20], UV/H_2O_2/Fe^{2+} [21] and UV/H_2O_2/$S_2O_8^{2-}$/Fe^{2+} [15, 18] processes are shown in reactions (1–14).

$$H_2O_2 + hv \rightarrow 2^{\cdot}OH, \quad (5)$$

$$2^{\cdot}OH \rightarrow H_2O_2, \quad (6)$$

$$S_2O_8^{2-} + hv \rightarrow 2SO_4^{\cdot-}, \quad (7)$$

$$S_2O_8^{2-} + {}^{\cdot}OH \rightarrow S_2O_8^{\cdot-} + OH^-, \quad (8)$$

$$S_2O_8^{2-} + H_2O_2 \rightarrow 2SO_4^{2-} + 2H^+ + O_2, \quad (9)$$

$$SO_4^{\cdot-} + {}^{\cdot}OH \rightarrow H^+ + SO_4^{2-} + 0.5O_2, \quad (10)$$

$$SO_4^{\cdot-} + SO_4^{\cdot-} \rightarrow S_2O_8^{2-}, \quad (11)$$

$$SO_4^{\cdot-} + S_2O_8^{2-} \rightarrow SO_4^{2-} + S_2O_8^{\cdot-}, \quad (12)$$

$$SO_4^{\cdot-} + H_2O \rightarrow SO_4^{2-} + {}^{\cdot}OH + H^+, \quad (13)$$

$$Fe^{2+} + S_2O_8^{2-} \rightarrow Fe^{3+} + SO_4^{\cdot-} + SO_4^{2-}. \quad (14)$$

Among the examined processes, the UV/H_2O_2/Fe^{2+} had the lowest mineralization efficiency. It can be attributed to the scavenging effect of $S_2O_8{}^{2-}$ on $^{\bullet}OH$ and H_2O_2 (reactions 8 and 9) which caused the reduction of the concentration of reactive radicals in the UV/H_2O_2/$S_2O_8{}^{2-}$ process rather than in the UV/H_2O_2 process. In the UV/H_2O_2/$S_2O_8{}^{2-}$ process, the Fe^{2+} catalyzed the decomposition of H_2O_2 to form more reactive radicals and, consequently, enhanced the mineralization efficiency; however, this was not the case with the UV/H_2O_2 process.

It can be argued that the UV/H_2O_2/$S_2O_8{}^{2-}$/Fe^{2+} process had the highest mineralization efficiency among all the investigated processes. Indeed, this process was a combination of UV/H_2O_2, UV/$S_2O_8{}^{2-}$, H_2O_2/Fe^{2+}, $S_2O_8{}^{2-}$/Fe^{2+}, UV/H_2O_2/Fe^{2+} and UV/H_2O_2/Fe^{2+}, which led to the efficient formation of reactive radicals and dye degradation.

The variations of solution pH in UV/H_2O_2, UV/H_2O_2/Fe^{2+}, UV/H_2O_2/$S_2O_8{}^{2-}$ and UV/H_2O_2/$S_2O_8{}^{2-}$/Fe^{2+} processes are shown in Fig. 1c. As can be seen in this figure, the solution pH in UV/H_2O_2 process decreased to 3.6 and then remained constant. The reduction in solution pH can be attributed to the production of organic acids during dye degradation. Furthermore, Fig. 1c depicts that in the UV/H_2O_2/Fe^{2+} process, first the solution pH decreased, and then increased with time. The increase in solution pH can probably be attributed to the Fenton reaction, which led to the production of OH^-, $^{\bullet}OH$ and Fe^{3+}. The increase in OH^- concentration resulted in an increase in the solution pH. In UV/H_2O_2/$S_2O_8{}^{2-}$ and UV/H_2O_2/$S_2O_8{}^{2-}$/Fe^{2+} processes, the solution pH decreased along with time, which was attributed to the production of H^+ through the reaction presented in reactions (2), (3), (9), (10), and (13). As illustrated in Fig. 1d, the decrease in concentration of H_2O_2 in UV/H_2O_2/$S_2O_8{}^{2-}$/Fe^{2+} process is faster than other processes. Since AR73 degradation in UV/H_2O_2/$S_2O_8{}^{2-}$/Fe^{2+} process was higher than other processes

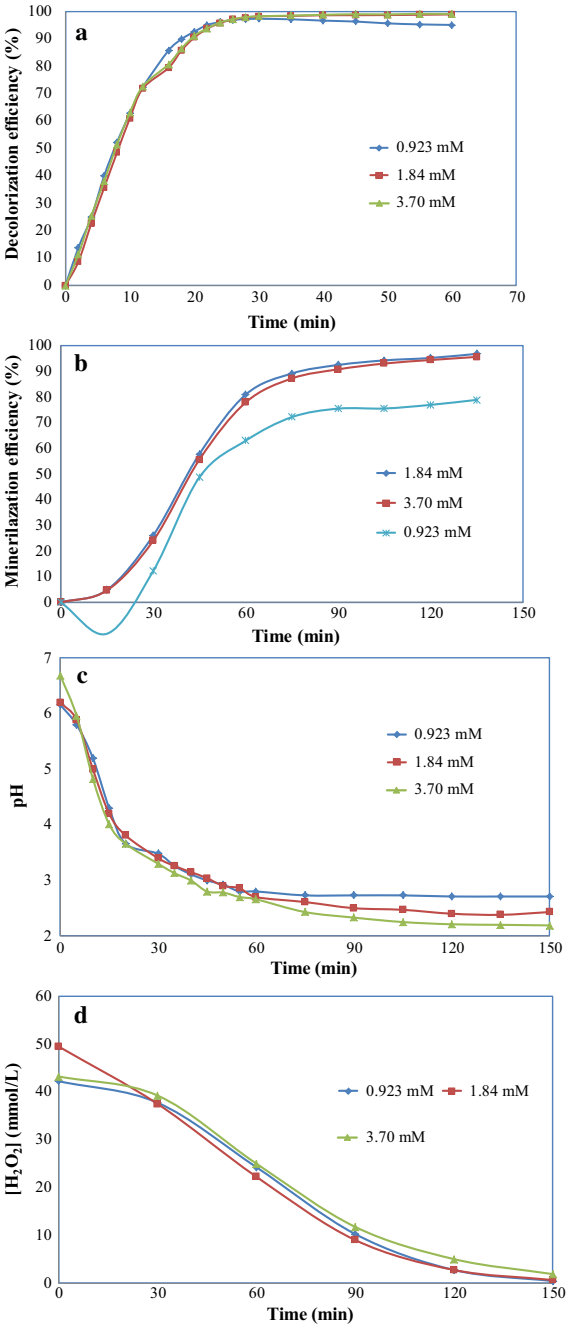

Fig. 2 Effect of initial concentration of $S_2O_8^{2-}$ on **a** decolorization efficiency, **b** mineralization efficiency, **c** pH of solution, and **d** H_2O_2 concentration during the treatment of AR73 solution by UV/H_2O_2/$S_2O_8^{2-}$/Fe^{2+} process in the presence of $[AR73]_0 = 0.1$ mM, $[H_2O_2]_0 = 44.4$ mM, and $[Fe^{2+}]_0 = 2.43$ mg/L

(Fig. 1b), it may be concluded that most of H_2O_2 in the UV/H_2O_2/$S_2O_8^{2-}$/Fe^{2+} process was used to produce $^{\bullet}OH$. So, the concentration of H_2O_2 decreased.

The effect of the initial $S_2O_8^{2-}$concentration in UV/H_2O_2/$S_2O_8^{2-}$/Fe^{2+} process

To investigate the effect of initial $S_2O_8^{2-}$ concentration on degradation efficiency of AR73, the researchers conducted UV/H_2O_2/$S_2O_8^{2-}$/Fe^{2+} experiments with different $S_2O_8^{2-}$ concentrations ranging from 0.923 to 3.70 mM for 150 min. when H_2O_2 and $FeSO_4$ concentrations and incident energy of the UV lamp were 44.4 mM, 12.05 mg/L, and 27 W/m^2, respectively. Figure 2 depicts the decolorization and mineralization profiles of AR73 solution and the variations of pH and H_2O_2 concentrations during the UV/H_2O_2/$S_2O_8^{2-}$/Fe^{2+} process. Figure 2a indicates that in the presence of all the examined $S_2O_8^{2-}$ concentrations, the UV/H_2O_2/$S_2O_8^{2-}$/Fe^{2+} process has the potential to decolorize the AR73 solution efficiently within 30 min. Figure 2b shows that the mineralization efficiency increases as the $S_2O_8^{2-}$ concentration increases up to 1.84 mM. This can be attributed to the increase in the development of reactive radicals and, thus, the enhancement of efficient mineralization of AR73. However, more increase in initial $S_2O_8^{2-}$ concentration led to a decrease in mineralization of AR73 due to contribution of developed radicals in other reactions rather than degradation of pollutant (Eqs. 10–12). The obtained results in Fig. 2c indicate that as the UV/H_2O_2/$S_2O_8^{2-}$/Fe^{2+} process proceeded, the solution pH decreased with an increase in the initial $S_2O_8^{2-}$ concentration due to the increase in the solution acidity. In other words, the reduction in the solution pH can be attributed to the production of organic acids through dye degradation and increase in H^+ concentration, which can be explained by the reactions (10) and (13). Further increase in initial $S_2O_8^{2-}$ concentration led to the further production of H^+ and further decrease in the solution pH. As shown in Fig. 2d, with increasing $S_2O_8^{2-}$concentration, H_2O_2 concentration decreases; however, there is no significant difference in decrease profiles of H_2O_2 concentration in the presence of different initial $S_2O_8^{2-}$concentrations.

The effect of Fe^{2+} immobilization on its catalytic activity in UV/H_2O_2/$S_2O_8^{2-}$/catalyst process

Catalytic formation of reactive radicals in the presence of Fe^{2+} is regarded as a promising method for degrading organic pollutants. In these processes, iron ions leave the solution in the form of iron-containing sludge. One way for overcoming this drawback is to immobilize Fe^{2+} on an appropriate surface to prepare a more stable heterogeneous catalyst. For examining the effect of Fe^{2+} immobilization on its catalytic performance, this cation was immobilized on the surface of ZSM5 zeolite to prepare heterogeneous Fe^{2+}–ZSM5 catalyst. The concentration of Fe^{2+} and Fe^{2+}–ZSM5 catalyst is, respectively, 2.66 mg/L and 236.6 mg/L. Moreover, it can be mentioned that the concentration of AR73 is 0.10 mM and the initial TOC of the solution is 26.5 mg/L. Decolorization and mineralization profile of AR73 solution in UV/H_2O_2/$S_2O_8^{2-}$/catalyst process are illustrated in Fig. 3a, b. Comparison of the obtained results reveals that the degradation efficiency in the Fe^{2+}

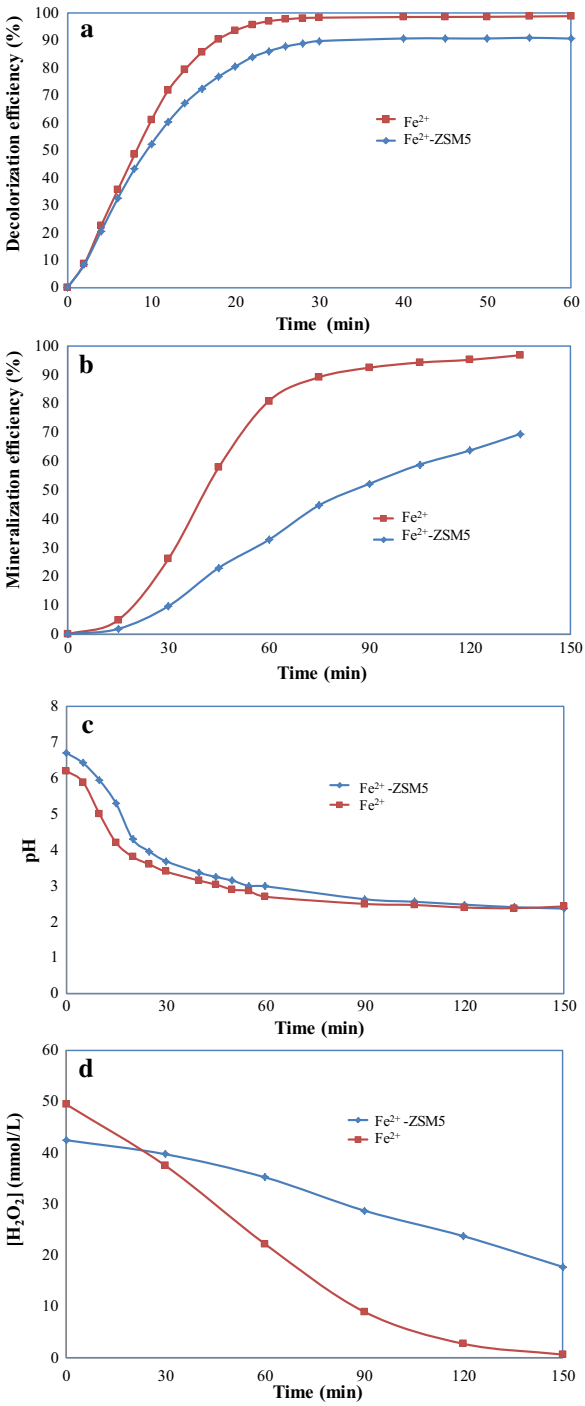

Fig. 3 Effect of Fe^{2+} immobilization on **a** decolorization efficiency, **b** mineralization efficiency, **c** pH of solution, and **d** H_2O_2 concentration during the treatment of AR73 solution by $UV/H_2O_2/S_2O_8^{2-}/Fe^{2+}$ processes

catalyzed process is higher than the Fe^{2+}–ZSM5 catalyzed process. This higher efficiency can be attributed to the mass transfer limitation of the heterogeneous catalytic systems, which decrease the adsorption of H_2O_2 and AR73 molecules on the surface of Fe^{2+}–ZSM5 where reactive radicals and dye degradation are formed [22]. Figure 3c indicates that the pH solution variations in UV/H_2O_2/$S_2O_8^{2-}$/Fe^{2+} and UV/H_2O_2/$S_2O_8^{2-}$/Fe^{2+}–ZSM5 are similar. However, H_2O_2 concentration during the UV/H_2O_2/$S_2O_8^{2-}$/Fe^{2+} process decreases more than that of the UV/H_2O_2/$S_2O_8^{2-}$/Fe^{2+}–ZSM5 process, which indicates the higher catalytic performance for the homogeneous catalyst rather than the heterogeneous one (Fig. 3d).

Conclusion

It can be concluded that: (1) in the presence of $S_2O_8^{2-}$ and UV light, Fe^{2+}/H_2O_2 is efficient in mineralizing azo dye, Acid Red 73, (2) an increase in the initial concentration of $S_2O_8^{2-}$ enhances the mineralization efficiency, and (3) Fe^{2+} immobilization decreases its catalytic performance in H_2O_2/$S_2O_8^{2-}$/catalyst/UV process.

Acknowledgments The authors thank the Université de Haute-Alsace (France) and University of Tabriz (Iran) for their support.

References

1. M. Sheydaei, S. Aber, A. Khataee, J. Mol. Catal. A: Chem. **392**, 229 (2014)
2. B. Vahid, A. Khataee, Electrochim. Acta **88**, 614 (2013)
3. B. Ayoubi-Feiz, S. Aber, A. Khataee, E. Alipour, J. Mol. Catal. A: Chem. **395**, 440 (2014)
4. B. Ayoubi-Feiz, S. Aber, A. Khataee, E. Alipour, Environ. Sci. Pollut. Res. **21**, 8555 (2014)
5. V.J.P. Vilar, S.M.S. Capelo, T.F.C.V. Silva, R.A.R. Boaventura, Catal. Today **161**, 228 (2011)
6. R.F.F. Pontes, J.E.F. Moraes, A. Machulek Jr, J.M. Pinto, J. Hazard. Mater. **176**, 402 (2010)
7. N. Daneshvar, A.R. Khataee, J. Environ. Sci. Health Part A **41**, 315 (2006)
8. R. Li, C. Yang, H. Chen, G. Zeng, G. Yu, J. Guo, J. Hazard. Mater. **167**, 1028 (2009)
9. C.R.A. Bertoncini, R. Meneghini, H. Tolentino, Spectrochim. Acta Part A **77**, 908 (2010)
10. J.D. Laat, H. Gallard, Environ. Sci. Technol. **33**, 2726 (1999)
11. D. Sannino, V. Vaiano, P. Ciambelli, L.A. Isupova, Catal. Today **161**, 255 (2011)
12. B. Ahmed, E. Limem, A. Abdel-Wahab, B. Nasr, Ind. Eng. Chem. Res. **50**, 6673 (2011)
13. G. Charlot, *Chimie Analytique Quantitative*, 6, ed. Masson, Paris, 1974
14. M.B. Kasiri, H. Aleboyeh, A. Aleboyeh, Appl. Catal. B **84**, 9 (2008)
15. I. Grčić, D. Vujević, N. Koprivanac, Chem. Eng. J. **157**, 35 (2010)
16. W. Chu, Y.R. Wang, H.F. Leung, Chem. Eng. J. **178**, 154 (2011)
17. S.E.H. Etaiw, D.I. Saleh, Spectrochim. Acta Part A **117**, 54 (2014)
18. X. Wang, L. Wang, J. Li, J. Qiu, C. Cai, H. Zhang, Sep. Purif. Technol. **122**, 41 (2014)
19. A.R. Khataee, O. Mirzajani, Desalination **251**, 64 (2010)
20. I. Velo-Gala, J.J. López-Peñalver, M. Sánchez-Polo, J. Rivera-Utrilla, Chem. Eng. J. **241**, 504 (2014)
21. M. Sheydaei, S. Aber, A. Khataee, J. Ind. Eng. Chem. **20**, 1772 (2013)
22. A.N. Soon, B.H. Hameed, Desalination **269**, 1 (2011)